Inhibition of Ice Crystal Growth by Synthetic Glycopolymers: Implications for the Rational Design of Antifreeze Glycoprotein Mimics

5 authors, including:

Matthew Gibson
The University of Warwick
77 PUBLICATIONS **1,670** CITATIONS

SEE PROFILE

Sebastian Spain
The University of Sheffield
23 PUBLICATIONS **501** CITATIONS

SEE PROFILE

Luca Albertin
French National Centre for Scientific Resea…
25 PUBLICATIONS **755** CITATIONS

SEE PROFILE

Neil R Cameron
Durham University
114 PUBLICATIONS **4,523** CITATIONS

SEE PROFILE

Inhibition of Ice Crystal Growth by Synthetic Glycopolymers: Implications for the Rational Design of Antifreeze Glycoprotein Mimics

Matthew I. Gibson,[†] Carl A. Barker, Sebastian G. Spain, Luca Albertin,[‡] and
Neil R. Cameron*

*Interdisciplinary Research Centre in Polymer Science and Technology, Department of Chemistry,
University of Durham, South Road, Durham, DH1 3LE, United Kingdom*

A series of structurally diverse polymers, containing either peptide or vinyl-derived backbones, was tested for ice recrystallization inhibition activity, which is commonly associated with antifreeze (glyco)proteins. It was revealed that only polymers bearing hydroxyl groups in the side chain could inhibit ice growth. Furthermore, well-defined glycopolymers were shown to have a small but significant recrystallization inhibition effect, showing that it may be possible to design antifreeze glycoprotein mimics based upon polymers derived from vinyl monomers.

Introduction

Since antifreeze glycoproteins (AFGPs, Figure 1) were discovered in the blood serum of Antarctic fish,[1] they have attracted interest as additives in cryopreservation,[2,3] cryomedicine,[4] as cell membrane diffusion moderators,[5] and even in frozen foods.[6,7] Their three main effects are noncolligative freezing point depression, dynamic ice shaping, and recrystallization inhibition (RI). Noncolligative freezing point depression is a thermal hysteresis (TH) effect, whereby the freezing point is lowered below its equilibrium value but the melting point remains unchanged. This allows the fish to survive in water at subzero temperatures, even if ice crystals from the environment are present in vivo. By the processes of adsorption-inhibition and step pinning, the ice crystal morphology is also changed. This results in hexaganol bipyramids or, at high degrees of overcooling, long, thin spicular crystals.

A thorough investigation by Nishimura et al.[8] concluded that a particular amino acid sequence and the presence of an *N*-acetylated aminosugar are required for TH activity. This was postulated to be due to the defined secondary structure, as determined by circular dichroism (CD) spectroscopy, adopted by the glycosylated polypeptide. However, these workers did not consider recrystallization inhibition behavior as a marker of antifreeze activity. RI is the ability of a compound to reduce the rate at which ice crystals grow in a polycrystalline wafer, resulting in smaller crystals for stronger acting compounds. It is displayed by AFGPs (and related compounds), which retard or stop the growth of ice crystals at subzero temperatures without influencing nucleation processes. In the absence of AFGPs, larger ice crystals grow at the expense of smaller ones, resulting in a larger mean crystal size. As far as we can determine, a complete study of the structural features required for RI behavior is lacking. The most extensive work in this area has been
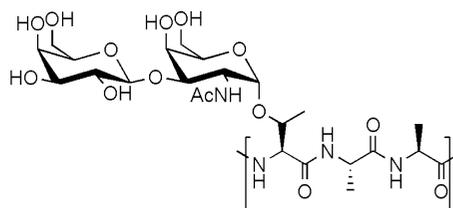
Figure 1. Structure of native AFGP.
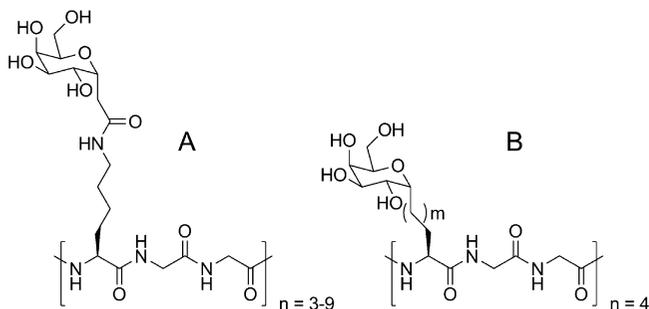
Figure 2. Structure of the *C*-linked analogues of Ben et al. (A) 1st generation; (B) 2nd generation, $m = 1-3$.

conducted by Ben et al. Their first generation AFGP mimics showed some RI activity, despite significant structural differences from native AFGP.[9–11] First, the disaccharide linked to threonine was replaced with a monosaccharide, galactose, linked to a lysine residue, and the two alanines were substituted by glycine (Figure 2A). These derivatives were only weakly active, approximately 80 times less so than AFGP 8, which is the least active of all the native AFGPs. Interestingly, the same molecules showed only weak dynamic ice shaping and thermal hysteresis effects, showing that it is possible to isolate the individual properties from one another. The importance of the distance between the carbohydrate moiety and the peptide backbone was probed by a second generation of RI inhibitors[9] (Figure 2B). The shortest distance of two CH_2 groups gave the strongest RI activity, while three and four CH_2 groups produced a sharp decrease similar to the G1 peptides described above. Galactose derivatives show far higher activity than glucose, possibly due to differences in their hydration level and thus interaction with supercooled water at the ice/water interface.[10] By isolating RI

* To whom correspondence should be addressed. E-mail: n.r.cameron@durham.ac.uk.

[†] Current address: Laboratoires des Polyméres, Institute des Materiaux, Ecole Polytechnique Fédérale de Lausanne, Station 12, Lausanne, CH-1100, Switzerland.

[‡] Current address: Centre de Recherches sur les Macromolécules Végétales, Domaine Universitaire de Grenoble St Martin d'Hères, 601 rue de la Chimie, France.

from TH/ice shaping activity, a significant caveat with using AF(G)Ps in cryopreservation is removed: that is, the propensity to form spicular ice crystals during freezing. These are a product of rapid ice growth and can result in mechanical damage and cell lysis.[11] However, this ice crystal growth has been exploited to increase cell death during cancer-cryosurgery in the presence of AFGP, resulting in increased cell death in the desired area around the tumor.[12]

Perhaps the most remarkable example of an RI inhibitor is the structurally simple polymer poly(vinyl alcohol), PVA. It possesses neither the polypeptide backbone nor the carbohydrate moiety thought to be essential for RI activity. In fact, PVA with a molecular weight of ~80000 Da was found to be as effective as an RI inhibitor as AFGP 8 at equal molar concentrations[13] (NB this represents a 30× increase in mass concentration of PVA relative to AFGP 8). Later studies[14,15] showed that PVA inhibits the same crystal faces as native AFGPs, resulting in the appearance of pyramidal faces that previously had only been associated with AFGPs.[16] A very weak, but definite, thermal hysteresis of 0.037 K was also observed. The most remarkable feature is PVA's lack of a rigid secondary structure, which is thought to be essential if a sufficiently hydrophobic face is to be presented following adsorption onto the ice crystal surface. Poly(tartar amides)[17] (and other polyols[18,19]), which contain rigid amide bonds (like polypeptides) as well as multiple -OH functionalities, were shown by wide-angle X-ray scattering (WAXS) and differential scanning calorimetry (DSC) to inhibit the growth of hexagonal ice. No thermal hysteresis or quantitative RI assays were undertaken, preventing comparison to the aforementioned systems.

The related compounds known as antifreeze proteins (AFPs) should also be mentioned briefly. AFPs that display strong RI behavior have been found in nature and have been designed systematically.[20,21] They all contain an ice binding hydrophilic face and a hydrophobic face, which makes the addition of further water molecules energetically unfavorable. AFPs contain various functional groups in the peptide side-chain, including carbohydrates, alcohols, and amines, whereas AFGPs only contain OH (carbohydrate) groups. The common feature of AFPs is a well-defined secondary structure, compared to AFGP analogues, which are largely unstructured (a crystal structure of an AFGP has yet to be published).

In summary, the structural features required for RI inhibition for both native AFGPs and synthetic polymers are not yet known. This is largely due to difficulties in synthesizing AFGPs, together with the focus on thermal hysteresis properties rather than recrystallization inhibition, which are now known to be independent effects. In this paper we describe the influence of backbone structure and side-chain functionality of a series of water-soluble polymers on RI behavior to determine the features that are essential for RI activity.

Experimental Section

General. Phosphate-buffered saline solutions were prepared using preformulated tablets (Sigma-Aldrich) in 200 mL of MilliQ water (>18 Ω mean resistivity) to give a buffered pH of 7.4. Poly(vinyl alcohol), poly(acrylic acid), poly(ethylene oxide), and poly(L-hydroxyproline) were all purchased from Sigma-Aldrich. Poly(2-aminoethyl methacrylate) was synthesized by the free radical polymerization of the hydrochloride salt of 2-aminoethyl methacrylate and characterized by size exclusion chromatography (SEC). Ice wafers were annealed on a Linkam THMS600 thermostatted microscope stage using liquid nitrogen as the coolant. NMR spectroscopy (^{1}H, ^{13}C, COSY, NOESY, HSQC) was conducted on either a Varian Inova 500 or a Bruker Avance 400

spectrometer operating at 500 and 400 MHz, respectively. Mass spectral analyses were preformed on a Micromass LCT spectrometer using positive or negative electrospray mode. Infrared spectroscopy was conducted on a Nicolet Nexus FT-IR spectrometer using samples prepared as KBr discs. SEC was performed using a Viscotek TDA 301 triple detection (with angular correction) SEC fitted with two (300 × 7.5 mm) GMPWxl methacrylate-based mixed bed columns having refractive index, viscometer, and RALLS detectors. For aqueous SEC, the eluent was 0.05 M NaNO$_3$ solution (80/20 v/v water/methanol) containing 2.5 mL/liter 1.0 M NaOH, at a flow rate of 1.0 mL/minute and at a constant temperature of 30 °C and calibrated with narrow polydispersity index (PDI) PEO standards. THF SEC was undertaken at a flow rate of 1.0 mL/minute and at a constant temperature of 30 °C and calibrated with narrow polydispersity index (PDI) polystyrene standards. Refractive index increments (dn/dc) were determined by injection of a known concentration of the polymer analyte in question.

Recrystallization Inhibition Assay. The method of Knight et al. was employed.[22] A 10 μL sample of polymer dissolved in PBS buffer (pH 7.4) was dropped 1.5 m down a hollow acrylic tube onto a piece of polished aluminum sat on dry ice. Upon hitting the aluminum, a wafer with diameter of approximately 10 mm was formed instantaneously. The wafer was transferred using a chilled blade to a glass slide onto the Linkam cool stage and held at −6 °C under N$_2$ for 30 min. Photographs through crossed polarizers, at a resolution of 2 megapixels, were taken of the initial wafer (to ensure that a polycrystalline sample had been obtained) and after 30 min. ImageJ was used to analyze the obtained images.[23] A number of the largest ice crystals (30+) in each wafers were measured and the single largest length in any axis recorded. This was repeated for at least three wafers and the average (mean) value was calculated to find the largest grain dimension along any axis. The average of this value from three individual wafers was calculated to give the mean largest grain size (MLGS).

Polypeptide Synthesis. The synthesis of well-defined poly(L-lysine·HBr) and poly(L-glutamate) sodium salt was achieved by the polymerization of ϵ-N-Boc-L-lysine (LysBoc) and γ-benzyl-L-glutamic acid (BLG) N-carboxyanhydrides (NCAs)[24,25] using a modified procedure. The NCAs were prepared from their corresponding N-Boc amino acids and purified by aqueous extraction as described previously.[26]

Poly(γ-benzyl-L-glutamate) (PBLG). BLG NCA (0.20 g, 0.75 mmol) was dissolved in 3 mL of dry dichloromethane (DCM) and injected into a pre-evacuated Schlenk tube, fitted with a Young's tap and a 9 mm rubber septum. The DCM was removed under vacuum and the NCA was allowed to dry under vacuum for an additional 2 h. THF (3 mL) was vacuum-distilled into the vessel to give an approximately 10% (wt) solution. The tube was then immersed in an oil bath thermostatted at 35 °C and stirred to dissolution. n-Hexylamine (0.08 mL, 0.2 M solution) was added via syringe into the tube, and the resulting solution was allowed to stir for 4 days.

Following this, a 100 μL sample was withdrawn for SEC analysis, and the remainder of the reaction was poured into a 10-fold excess of diethyl ether with stirring, and the resulting white powder collected by filtration. Further purification was achieved by redissolving in THF and precipitating into a 10-fold excess of water. Yield 0.13 g, 75%. ^{1}H NMR (500 MHz; CDCl$_3$) δ_{ppm} 7.19−7.29 (5H, Ar), 5.04 (2H, CO$_2$C**H**$_2$), 3.94 (1H, NHC**H**), 2.60 (2H, C**H**$_2$CO$_2$), 2.28 (2H, C**H**$_2$CH$_2$CO$_2$). ^{13}C NMR (125 MHz; CDCl$_3$) δ_{ppm} 175, 172, 136, 128, 128.4, 66, 57, 31, 25. SEC (THF): dn/dc = 0.102 mL/g, M_n = 19000, M_w/M_n (PDI) = 1.30.

Poly(L-glutamate) Sodium Salt. PBLG (250 mg, 1.16 mmol repeating unit) was dissolved in 1 mL of trifluoroacetic acid. HBr (33% in acetic acid) (0.54 mL, 2.9 mmol) was added dropwise under N$_2$ and the resulting solution was stirred at room temperature for 1 h. The solution was then precipitated into a 30 fold excess of diethyl ether. The solid was washed (2 × 10 mL) with diethyl ether, dissolved in 2 mL of 0.5 M aqueous NaOH solution, and dialyzed against distilled water. The polymer was obtained as a white solid by freeze-drying.

Yield 145 mg, 72%. ^{1}H NMR (500 MHz; CDCl$_3$) δ_{ppm} 1.72 (1H, CH$_2$CH$_2$CO$_2$), 1.83 (1H, CH$_2$CH$_2$CO$_2$), 2.07 (2H, CH$_2$CO$_2$), 4.11 (1H, NHCH). ^{13}C NMR (125 MHz; CDCl$_3$) δ_{ppm} 28.2, 33.7, 53.6, 173.6, 181.6.

Poly(ε-*N*-butoxycarbonyl-L-lysine) (PLysBoc). The same procedure was used as with the polymerization of BLG NCA, using DMAc as the solvent, LysBoc NCA (0.2 g, 7.35mmol), and *n*-hexylamine (0.08 mL, 0.2 M solution). Yield 0.114 g, 68%. ^{1}H NMR (400 MHz; CDCl$_3$) δ_{ppm} 1.37 (13H, C(CH$_3$)$_3$ + CHCH$_2$CH$_2$ + CH$_2$CH$_2$NHBoc), 1.86 (2H, CHCH$_2$), 3.02 (2H, CH$_2$NHBoc), 5.14 (1H, NHCH), 8.21 (1H, NHBoc). ^{13}C NMR (100 MHz; CDCl$_3$) δ_{ppm} 21.5, 28.5, 29.7, 30.1, 40.5, 65.8, 78.7, 156.1, 170.7. SEC (THF): dn/dc = 0.05 mL/g, M_n = 13500, PDI = 1.37.

Poly(L-lysine·HBr). PLysBoc (160 mg, 0.66 mmol repeating unit) was dissolved in 1 mL of trifluroacetic acid·HBr (33% in acetic acid; 0.54 mL, 2.9 mmol), and the resulting solution was added dropwise under N$_2$ and stirred at room temperature for 1 h. The solution was then precipitated into a 30-fold excess of diethyl ether. The obtained solid was washed (2 × 10 mL) with diethyl ether, dissolved in distilled water, and dialysed against distilled water. The polymer was obtained as a white solid by freeze-drying. Yield 120 mg, 82%. ^{1}H NMR (400 MHz; CDCl$_3$) δ_{ppm} 1.20−2.82 (6H, CHCH$_2$ + CHCH$_2$CH$_2$ + CH$_2$CH$_2$NH$_2$), 2.81 (1H, CH$_2$NH$_2$), 4.11 (1H, NHCH). ^{13}C NMR (100 MHz; CDCl$_3$) δ_{ppm} 22.3, 26.5, 30.7, 39.3, 53.5, 173.7.

Glycopolymer Synthesis. RAFT polymerization of unprotected glycomonomers in aqueous solution was utilized to synthesize the well-defined glycopolymers used in this study. The monomers GalEMA[27] and MAMGlc[28] were synthesized as described previously.

Poly(methyl-6-*O*-methacryloyl-α-D-glucopyranoside) (PMAM-Glc). The monomer solution (8.00 mL, 8.00 mmol, HPLC water) was introduced into a Schlenk tube and mixed with ethanol solutions of 4,4′-azobis-(4-cyanopentanoic acid) (6.22 × 10^{-2} M, 1.300 mL, 8.08 × 10^{-5} mol) and (4-cyanopentanoic acid)-4-dithiobenzoate (5.18 × 10^{-1} M, 0.345 mL, 1.79 × 10^{-4} mol). The tube was degassed with four freeze−evacuate−thaw cycles and transferred to a water bath preheated to 70 °C. After 50 min, the reaction was stopped by cooling in ice−water (5 min). The polymer was recovered by precipitation in excess ethanol followed by centrifugation and freeze-drying (overnight, dark). Yield 1.10 g, 53%. NMR data were in accord with values reported previously.[28] SEC (aqueous): dn/dc = 0.098 mL/g, M_n = 9500, PDI = 1.09.

Poly((β-D-galactosyloxy)ethyl methacrylate), pGalEMA. To a solution of GalEMA (100 mg, 0.348 mmol) in UHQ water was added (4-cyanopentanoic acid)-4-dithiobenzoate (7 μmol) and 4,4′-azobis(4-cyanopentanoic acid) (3.5 μmol) as 16 mg mL^{-1} solutions in absolute ethanol. The solution was degassed by three freeze−pump−thaw cycles and purged with nitrogen before sealing. The solution was stirred at 70 °C for 3 h then dialyzed and lyophilized to yield pGalEMA as a hygroscopic pink solid. Yield 65 mg, 65%. NMR data were in accord with values reported previously.[29] SEC (aqueous): dn/dc = 0.153 mL/g, M_n = 12700, PDI = 1.03.

Results and Discussion

To investigate the structural features required for recrystallization inhibition behavior, a series of structurally diverse water-soluble polymers were selected. The polymers are shown in Scheme 1, and their structures are compared to that of the repeat unit of native AFGP.

High molecular weight (115000 Da) PVA was used as a positive control and neat PBS solution was used as a negative control. The results of RI experiments using these are shown in Table 1. The small range of values demonstrates the reproducibility of the RI assay, with only a small number of measurements (three). Details of this method are given in the Experimental Section: essentially, 10 μL of polymer solution was dropped onto an aluminum slide resting on dry ice. The

Scheme 1. Structures of the Polymers Evaluated in this Study for Recrystallization Inhibition Activity
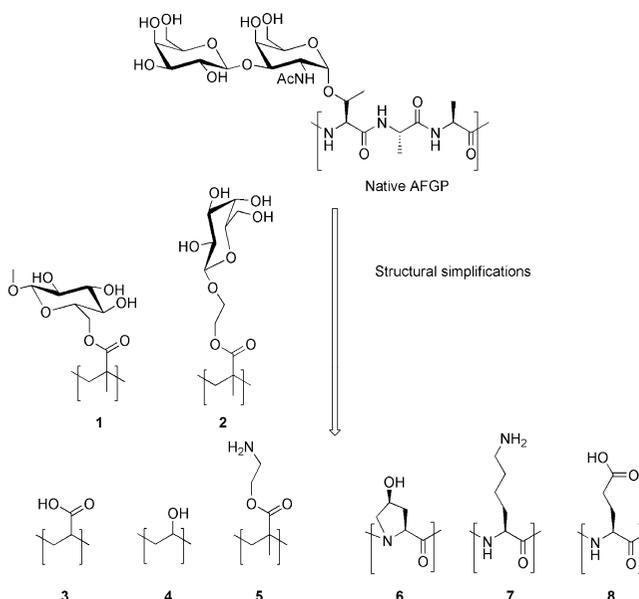
Table 1. Calculation of the Mean Largest Grain Sized (MLGS) from Three Individual Ice Wafers Containing Either Neat PBS (pH 7.4) or PVA$_{2625}$[a]

	LGS 1	LGS 2	LGS 3	MLGS[c]	1/2 range
PBS	272.7	268.3	254.3	265.1	9.6
PVA$_{2625}$[b]	55.0	48.7	54.4	52.7	3.5

[a] All measurements are in μm. [b] Concentration = 5 mg mL^{-1}. [c] Mean of three measurements.

formed ice wafer was transferred to a cold stage and allowed to anneal (under N$_2$) for 30 min before being photographed. This method effectively separates the nucleation and growth processes. Thus, the influence of the polymers on ice recrystallization (growth) can be quantified by the size of the largest ice crystals after a fixed time period (30 min here). A large number of ice crystals in each image were measured to find the largest axis-length present, and the mean was calculated from three separate wafers. Figure 3 shows some typical micrographs. Other methods for measuring RI behavior exist but may not allow for quantitative comparisons between polymers,[17,30] thus, they were not employed here.

Influence of Side-Chain Functionality. Encouraged by the strong RI activity of PVA, we decided to probe the effect on RI activity of different side-chain functionality in water-soluble carbon-backbone polymers. The polymers employed are listed in Table 2.

The polymers were chosen in order to relate the RI properties to the charges on the side chains (i.e., positive, negative, or neutral). PEG is a neutral, water-soluble polymer that is isomeric to PVA and that possesses no side-chain functionality. The results of the assays for these polymers are summarized in Figure 4.

All three PVA chain lengths displayed RI behavior in agreement with a previous study, with PVA$_{2625}$ and PVA$_{205}$ both giving MLGS around 50 μm, which is the limit of detection by this method.[13] At equal molar concentrations, the high molecular weight PVA gave a stronger RI effect (smaller grains). At equal mass concentration (5 mg·mL^{-1}) the same relationship was seen: RI effect increased with molecular weight. By analyzing the data this way, it is possible to rule out any false positive results that might occur due to the high concentration of side
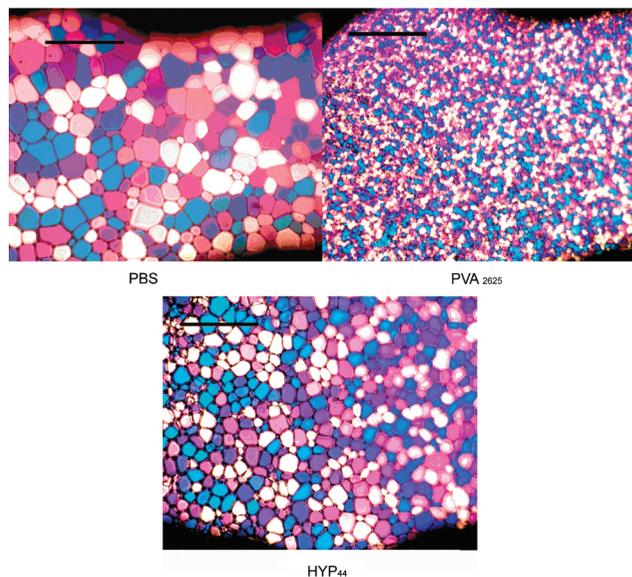
Figure 3. Optical micrographs, through crossed polarizers, of "splat" tested PBS, poly(vinyl alcohol) (PVA$_{2625}$; 5 mg·mL^{-1}) and poly(L-hydroxyproline) (HYP$_{44}$; 40 mg·mL^{-1}) solutions. Scale bar = 500 μm. Samples annealed at −6 °C for 30 min.

Table 2. Vinyl-Derived Polymers and their Characteristics[a]

polymer	M_w[b]	side chain functionality
(3)−PAA$_{54}$	5110	CO$_2$H
(5)−PAEM$_{135}$	20000	CO$_2$(CH$_2$)$_2$NH$_2$
(4)−PVA$_{2625}$	115500	OH
(4)−PVA$_{205}$	9000	OH
(4)−PVA$_{80}$	3500	OH
PEG$_{225}$	10000	N/A

[a] PAA = poly(acrylic acid); PAEM = poly(2-aminoethyl methacrylate); PVA = poly(vinyl alcohol); PEG = poly(ethylene glycol). Numbers in parenthesis indicate the structures in Scheme 1. [b] According to manufacturer's specifications. PDI values were not supplied by the manufacturer.
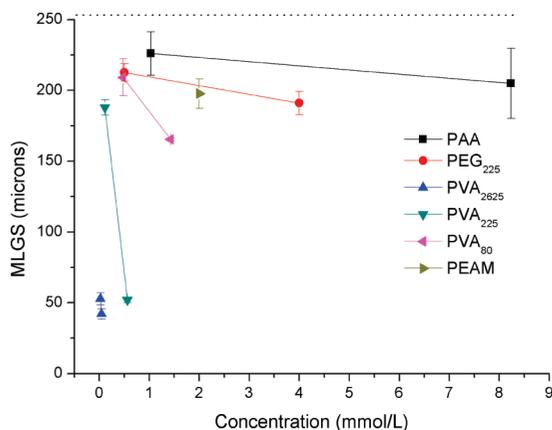
Figure 4. MLGS of the polymers shown in Table 2. Dashed line indicates PBS control. PEAM could not be used at higher concentrations due to gelation.

chain groups, when comparing polymers of different molecular weight, but at equal molar concentrations.[31] An important issue raised from this analysis is that both molar and mass concentrations should be considered when defining the activity of new polymers. This is especially true when comparing polymers of different structures, where equal molar concentrations can result in markedly different mass concentrations. The other polymers tested, PAA, PEAM, and PEG, all showed a small RI effect, in that they reduce the size of the crystals from 250 μm for PBS to around 200 μm in all cases. This does not appear to be a

Table 3. Polypeptides Used and their Molecular Characteristics

polymer	M_n[a]	PDI[a]	side chain
(7)−K$_{50}$	7200	1.37	(CH$_2$)$_4$NH$_2$
(7)−K$_{110}$	14400	1.34	(CH$_2$)$_4$NH$_2$
(8)−E$_{110}$	15900	1.23	(CH$_2$)$_2$CO$_2$H
(6)−HYP$_{44}$	5676[b]	[c]	OH

[a] Determined by SEC of the protected polymers. [b] Value from supplier. [c] Value not provided by supplier; K_x = poly(L-lysine); E_x = poly(L-glutamic acid); HYP$_x$ = poly(L-hydroxyproline).
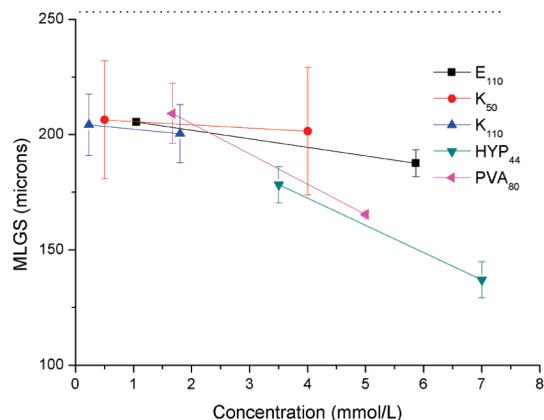
Figure 5. RI inhibition by peptide-based polymers. Dashed line indicates PBS control.

true RI effect, as PEG has previously been analyzed and has been shown to have no activity. Increasing the concentration of PAA to 40 mg·mL^{-1} (data not shown) did not give any significant decrease in the grain size. Finally, upon dilution there was no large increase in the grain size, as would be expected for polymers showing RI activity. Therefore, this apparent decrease in grain size could be attributed to the increased concentration of solutes in the case of the polymer electrolytes (which were used as their salts). These observations are important to avoid false positive (if rather weak) effects.

To investigate the role of solutes on RI, a 10 mg·mL^{-1} solution of 1-*O*-methyl-α-glucoside was analyzed. The observed MLGS was 198 μm, a similar value to that obtained for the polyelectrolytes, suggesting that additive effects due to increased numbers of solutes should be considered during interpretation of any results.

Homopolypeptide RI Activity. The polypeptide backbone of native AFGP is thought to play a role in its RI activity; therefore, it is prudent to investigate the RI properties of polypeptides with the same (or closely related) side chains as are present in the vinyl polymers, discussed in the previous section. A small range of polymers was synthesized from their corresponding *N*-carboxyanhydrides. The polymers shown in Table 3 were used for this study.

The polypeptides bearing charged side groups did not display any significant RI behavior, even at concentrations of 40 mg·mL^{-1} (Figure 5). The observations confirm the previous results that charged side chains, as the water solubilizing component, do not result in any RI. Conversely, the relatively low molecular weight poly(L-hydroxyproline)$_{44}$ showed a reasonably strong RI effect. Figure 5 also includes data for PVA$_{80}$, which has a similar molecular weight to the poly(L-hydroxyproline), shown in Figure 1, used here and, surprisingly, the observed RI activity of the two polymers is very similar. Poly(L-hydroxyproline) is expected to have a poly(L-proline)-type helical secondary structure,[32] but this does not give any significant increase in RI activity relative to the largely

Table 4. Molecular Characteristics of the Glycopolymers Used

polymer	$M_n{}^a$	$M_w/M_n{}^a$
(1)−PMAMGlc$_{70}$	18000	1.12
(1)−PMAMGlc$_{144}$	37000	1.05
(1)−PMAMGlc$_{220}$	56500	1.03
(1)−PMAMGlc$_{405}$	105000	1.24
(2)−PGalEMA$_{45}$	12700	1.30

^{a} Determined by aqueous SEC using a RALLS detector. Values in parentheses indicate the structures in Scheme 1. PMAMGlc = poly(methyl-6-*O*-methacryloyl-α-glucopyranoside). PGalEMA = poly((β-D-galactosyloxy)ethyl methacrylate).
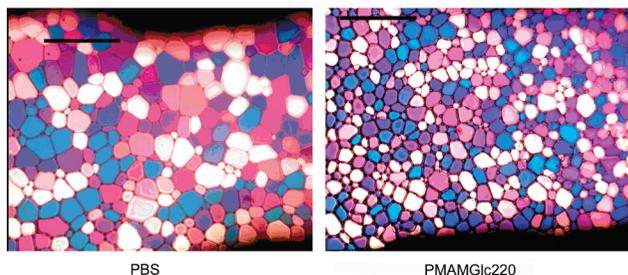
Figure 6. Optical micrograph of PBS (left) and PMAMGlc$_{220}$ at 40 mg·mL^{-1}. Scale bar represents 500 μm.

unstructured PVA and is significantly different to the secondary structure of native AFGP. The lack of activity for the charged side-chain polypeptides suggests that a rigid backbone of defined primary structure is not essential for RI activity, however, it may play a role in the increased RI activity of native AFGPs. No quantitative study using poly(L-hydroxyproline) has been described previously in the literature.

Carbon Backbone Glycopolymer RI Activity. The strong recrystallization inhibition observed with simple polyols encouraged us to investigate whether vinyl-derived glycopolymers would be similarly effective. The increased density of hydroxyl groups should facilitate stronger ice lattice binding, while the activity of PVA shows that a carbon-based backbone presents a sufficiently hydrophobic surface to produce RI behavior. Two structurally different glycopolymers of controlled molecular weight synthesized by aqueous RAFT polymerization of the appropriate monomer were tested (see Experimental Section for further details)[28] and are detailed in Table 4.

For these polymers, a high initial concentration corresponding to 40 mg·mL^{-1} was used to ensure that any effects were as pronounced as possible, avoiding any false negative results arising from weak activity. The micrographs in Figure 6 show a PBS control sample alongside PMAMGlc$_{220}$ at a concentration of 40 mg·mL^{-1}. The sample containing the polymer clearly shows a higher population of crystals and, hence, a smaller grain size. There are also no single large crystals in view, compared to the PBS, which contains several significantly larger crystals.

The data presented in Figure 7 show a strong correlation between both the concentration of the polymer solution and the molecular weight of the polymer with the observed MLGS. Both low molecular weight polymers (PMAMGlc$_{70}$ and PGalEMA$_{45}$) show similar behavior despite the differences in stereochemistry and linker to the polymer backbone. The observed largest grain size of 138 μm for the most active glycopolymer, PMAMGlc$_{410}$ at 0.44 mmol·L^{-1}, represents stronger activity than was observed for PVA$_{80}$ (M_w = 3500) but weaker than PVA$_{200}$ (M_w = 9000) at similar concentrations. Surprisingly, all the PMAMGlc samples displayed stronger RI activity than PVA$_{80}$. At the lower concentration of 0.11 mmol·L^{-1} PMAMGlc$_{410}$ retains its RI activity better than PVA$_{200}$ (MLGS of 171 μm compared to 188 μm). It should be noted that the total mass of glycopolymer is
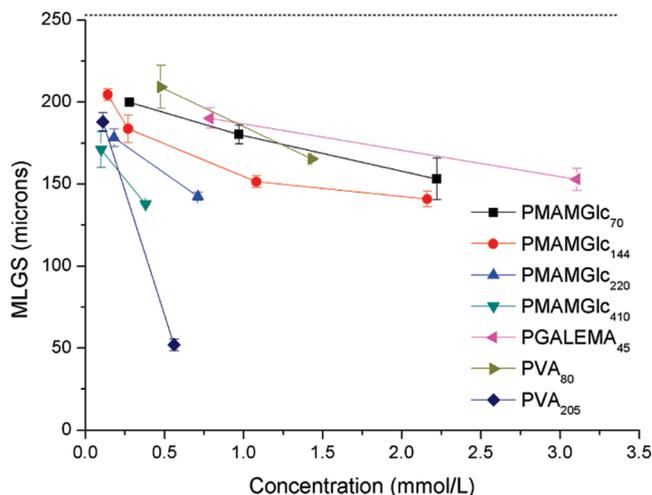
Figure 7. Change in MLGS with concentration for the vinyl-derived glycopolymers together with PVA for comparison. Dashed line indicates PBS control.
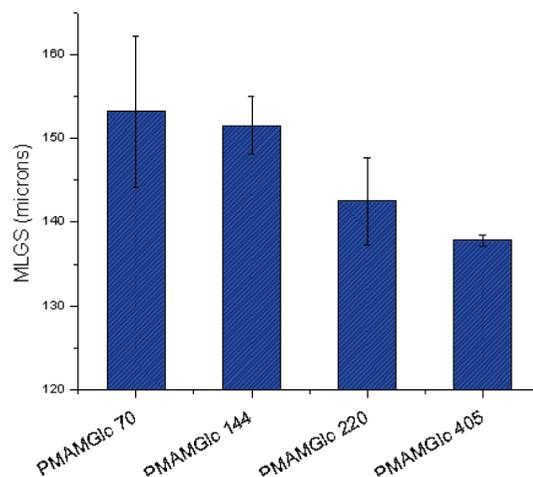
Figure 8. MLGS of PMAMGlc of varying molecular weight at a constant concentration of 40 mg·mL^{-1}. Error bars indicate the standard deviation.

far higher than the mass of PVA at equal molar concentrations. These observations are not due to colligative effects, as demonstrated by the fact that, at equal molar concentrations, the higher molecular weight polymers are more active than the lower. It is, however, necessary to explore whether the RI is affected by the total amount of carbohydrate present in the solution: that is, to see whether there are additive effects. This is done by comparing the results of the RI assays with polymers of equal mass concentration, rather than equal molar concentration. In this situation, the total number of repeat units is equal and the effects of polymer chain length can be probed.

In Figure 8, the results of the RI assay at 40 mg·mL^{-1} are shown for four different molecular weights of PMAMGlc. There is a clear trend toward increasing activity (decreasing grain size) with an increase in the molecular weight of the polymer. As the total carbohydrate concentration is constant throughout this series, the increase in activity can be attributed directly to the effect of increased chain length. This result is remarkable, considering the major structural differences between the glycopolymers and native AFGP. However, it should be noted that the activities observed are significantly lower than those of native AFGPs. The lowest molecular weight species, AFGP 8, is more active than these polymers even at concentrations as low as 10^{-3} mmol·L^{-1}.

It has previously been shown that hydroxyl groups are essential for thermal hysteresis in native AFGPs: oxidation to carboxylic acids results in complete loss of activity, but this has not been investigated with regard to recrystallization inhibition.[1,33] Our results show that RI activity of synthetic polymers is also dependent upon the presence of hydroxyl groups rather than other water-soluble motifs, which will have importance for the design of new AFGP mimics. Taking this into account, we can consider the increased activity of PVA relative to our glycopolymers at various chain lengths. We would expect that an increased concentration of -OH groups in the glycopolymer would increase the strength of the ice binding relative to PVA and, consequently, increase the RI activity. In fact, this is the opposite of what is observed. Previous work by Ben et al. indicates that a short distance between polypeptide backbone and the carbohydrate moiety in their AFGP mimics is crucial to maintaining RI function.[9] Increasing the separation from two CH_2 units to four resulted in a complete loss of RI activity. The separation from backbone to -OH in PVA is zero units, whereas in PMAMGlc it is three atoms and in PGalEMA it is five atoms. This would explain the reduced RI activity of the glycopolymers relative to PVA when the mode of action is assumed to follow the absorption-inhibition model. The short separation in PVA would result in the hydrophobic poly(vinyl) backbone being presented close to the advancing ice front, causing more effective inhibition. In the case of the glycopolymers, the long, flexible linker would allow more backbone flexibility to avoid contact with the hydrophilic ice surface and, thus, effect less efficient inhibition. This insight suggests that design concepts for peptide AFGP mimics can also be applied to polymeric mimics. Comparison with the conformation of native AFGP is difficult, owing to the complex secondary structures assumed by peptides. In contrast, the glycopolymers studied here have been found by circular dichroism spectroscopy to adopt a random coil conformation in solution (data not shown).

Conclusions

In the present study, the effect of a small library of water-soluble polymers on the recrystallization of ice was investigated. The results from carbon and peptide backbone polymers show that the hydroxyl group is essential for activity, whereas the polymer backbone is more tolerant to modifications. However, the data presented here do not rule out, or measure, the contribution from the backbone and the relative conformation, which may be significant. In particular, the RI activity of poly(L-hydroxyproline) was assessed in a quantitative fashion for the first time. Carboxylic acid and amine containing polymers displayed no tendency for RI activity. When this information is used, synthetic glycopolymers bearing glucose and galactose derived moieties were assayed. Amazingly, they also show a measurable RI effect. This is significant, as previous studies have shown that even small changes in the structure of native AFGP results in complete loss of RI behavior.[8] Critically, the reduced activity of the glycopolymers relative to PVA indicates that the density of the hydroxyl groups is less important than their distance from the polymer backbone. The glycopolymers show a strong molecular weight dependence on the RI effect, with the higher molecular polymers being more active.

While the polymers tested in this study are neither as active as the native AFGP, nor the rationally designed peptide-mimics of Ben et al.,[9] they do provide an important insight into this intriguing process. By demonstrating that vinyl-based polymers can inhibit ice growth, we anticipate that more active compounds can be created using the wealth of well-established controlled polymerization techniques. These methods are more suited to large scale production than solid-phase peptide synthesis and a plethora of polymerizable, hydroxy containing monomers are available. Potential applications of such systems include cryo-protectants and frozen food texture improvers.

References and Notes

(1) Harding, M. M.; Anderberg, P. I.; Haymet, A. D. J *Eur. J. Biochem.* **2003**, *270*, 1381–1392.

(2) Palasz, A. T.; Mapletoft, R. J. *Biotech. Adv.* **1996**, *14*, 127–149.

(3) Prathalingam, N. S.; Holt, W. V.; Revell, S. G.; Mirczuk, S.; Fleck, R. A.; Watson, P. F. *Theriogenology* **2006**, *66*, 1894–1900.

(4) Bouvet, V.; Ben, R. N. *Cell. Biochem. Biophys.* **2003**, *39*, 133–144.

(5) Inglis, S. R.; Turner, J. J.; Harding, M. M. *Curr. Protein Pept. Sci.* **2006**, *7*, 509–522.

(6) Griffith, M.; Ewart, K. V. *Biotech. Adv.* **1995**, *13*, 375–402.

(7) Crevel, R. W. R.; Fedyk, J. K.; Spurgeon, M. J. *Food Chem. Toxicol.* **2002**, *40*, 899–903.

(8) Tachibana, Y.; Fletcher, G. L.; Naoki, F.; Tsuda, S.; Monde, K.; Nishimura, S.-I. *Angew. Chem., Int. Ed.* **2004**, *43*, 856–862.

(9) Liu, S.; Ben, R. N. *Org. Lett.* **2005**, *7*, 2385–2388.

(10) Czechura, P.; Tam, R. Y.; Dimitrijevic, E.; Murphy, A. V.; Ben, R. N. *J. Am. Chem. Soc.* **2008**, *130*, 2928–2929.

(11) Mugnano, J. A.; Wang, T.; Layne, J. R.; Devries, A. L.; Lee, R. E. *Am. J. Physiol.* **1995**, *38*, R474–R479.

(12) Koushafar, H.; Pham, L.; Lee, C.; Rubinsky, B. *J. Surg. Oncol.* **1997**, *66*, 114–121.

(13) Inada, T.; Lu, S.-S. *Cryst. Growth Des.* **2003**, *3*, 747–752.

(14) Inada, T.; Lu, S.-S. *Chem. Phys. Lett.* **2004**, *394*, 361–365.

(15) Inada, T.; Modak, P. R. *Chem. Eng. Sci.* **2006**, *61*, 3149–3158.

(16) Ewart, K. V.; Lin, Q.; Hew, C. L. *Cell. Mol. Life Sci.* **1999**, *55*, 271–283.

(17) Yagci, Y. E.; Antonietti, M.; Borner, H. G. *Macromol. Rapid Commun.* **2006**, *27*, 1660–1664.

(18) Baruch, E.; Mastai, Y. *Macromol. Rapid Commun.* **2007**, *28*, 2256–2261.

(19) Mastai, Y.; Rudloff, J.; Colfen, H.; Antonietti, M. *Chem. Phys. Chem.* **2002**, *1*, 119–123.

(20) Zhang, W.; Laurson, R. A. *FEBS Lett.* **1999**, *455*, 372–376.

(21) Wierzbicki, A.; Knight, C. A.; Rutland, T. J.; Muccio, D. D.; Pybus, B. S.; Sikes, C. S. *Biomacromolecules* **2000**, *1*, 268–274.

(22) Knight, C. A.; Hallet, J.; DeVries, A. L. *Cryobiology* **1988**, *25*, 55–60.

(23) Rasband, W. S. *Image J*, version 1.37; National Institutes of Health: Bethesda, Maryland, 1997−2006. http://rsb.info.nih.gov/ij/.

(24) Rodriguez Hernandez, J.; Klok, H.-A. *J. Polym. Sci., Part A: Polym. Chem.* **2003**, *41*, 1167–1187.

(25) Aliferis, T.; Iatrou, H.; Hadjichristidis, N. *Biomacromolecules* **2004**, *5*, 1653–1656.

(26) Poche, D.; Moore, M. J.; Bowles, J. L. *Synth. Commun.* **1999**, *29*, 843–854.

(27) Ambrosi, M.; Batsanov, A. S.; Cameron, N. R.; Davis, B. G.; Howard, J. A. K.; Hunter, R. *J. Chem. Soc., Perkin Trans.* **2002**, *1*, 45–52.

(28) Albertin, L.; Cameron, N. R. *Macromolecules* **2007**, *40*, 6082–6093.

(29) Spain, S. G.; Albertin, L.; Cameron, N. R. *Chem. Commun.* **2006**, 4198–4200.

(30) Tomczak, M. M.; Marshall, C. B.; Gilbert, J. A.; Davies, P. L. *Biochem. Biophys. Res. Commun.* **2003**, *311*, 1041–1046.

(31) Eniade, A.; Purushotham, M.; Ben, R. N.; Wang, J. B.; Horwath, K. *Cell. Biochem. Biophys.* **2003**, *38*, 115–124.

(32) Horng, J. C.; Raines, R. T. *Protein Sci.* **2006**, *15*, 74–83.

(33) Komatsu, S. K.; Devries, A. L.; Feeney, R. E. *J. Biol. Chem.* **1970**, *245*, 2909.